Molecular Therapy
Original Article

Macrophage-Derived mir-155-Containing Exosomes Suppress Fibroblast Proliferation and Promote Fibroblast Inflammation during Cardiac Injury

Chunxiao Wang,[1,2,3] Congcong Zhang,[1,2,3] Luxin Liu,[1,2,3] Xi A,[1,2,3] Boya Chen,[1,2,3] Yulin Li,[1,2,3] and Jie Du[1,2,3]

[1]Beijing Anzhen Hospital, Capital Medical University, Beijing 100029, China; [2]The Key Laboratory of Remodeling-Related Cardiovascular Diseases, Ministry of Education, Beijing 100029, China; [3]Beijing Institute of Heart Lung and Blood Vessel Diseases, Beijing Collaborative Innovative Research Center for Cardiovascular Diseases, Beijing 100029, China

Inflammation plays an important role in cardiac injuries. Here, we examined the role of miRNA in regulating inflammation and cardiac injury during myocardial infarction. We showed that mir-155 expression was increased in the mouse heart after myocardial infarction. Upregulated mir-155 was primarily presented in macrophages and cardiac fibroblasts of injured hearts, while pri-mir-155 was only expressed in macrophages. mir-155 was also presented in exosomes derived from macrophages, and it can be transferred into cardiac fibroblasts by macrophage-derived exosomes. A mir-155 mimic or mir-155 containing exosomes inhibited cardiac fibroblast proliferation by downregulating Son of Sevenless 1 expression and promoted inflammation by decreasing Suppressor of Cytokine Signaling 1 expression. These effects were reversed by the addition of a mir-155 inhibitor. In vivo, mir-155-deficient mice showed a significant reduction of the incidence of cardiac rupture and an improved cardiac function compared with wild-type mice. Moreover, transfusion of wild-type macrophage exosomes to mir-155$^{-/-}$ mice exacerbated cardiac rupture. Finally, the mir-155-deficient mice exhibited elevated fibroblast proliferation and collagen production, along with reduced cardiac inflammation in injured heart. Taken together, our results demonstrate that activated macrophages secrete mir-155-enriched exosomes and identify macrophage-derived mir-155 as a paracrine regulator for fibroblast proliferation and inflammation; thus, a mir-155 inhibitor (i.e., mir-155 antagomir) has the potential to be a therapeutic agent for reducing acute myocardial-infarction-related adverse events.

INTRODUCTION

MicroRNAs (miRNAs), a novel class of small non-coding RNAs, are implicated in the pathogenesis of various cardiovascular diseases and regarded as an intriguing target for therapeutic intervention.[1] miRNAs downregulate the expression of messenger RNA targets having related functions, which consequently govern intricate biological processes.[2] Recently, several studies have shown that miRNAs are packaged into exosomes. As a kind of paracrine messenger, exosomes mediate the cell-cell communication.[3,4] Exosomes are membranous vesicles with a diameter <100 nM.[5,6] They are mainly formed from the inward budding of multi-vesicular bodies and are shed from both healthy and diseased cells.[7] Exosomes contain abundant miRNAs, mRNAs, proteins, or even organelles derived from donor cells that are transferred into specific target cells.[8,9] Some miRNAs can be packaged into monocyte- and macrophage-derived exosomes and to regulate the function of recipient cells.[10] For example, secreted monocytic mir-150 enhances targeted endothelial cell migration,[11] while macrophage-derived mir-223-containing exosomes induce macrophage differentiation,[12] suggesting that macrophages release miRNA-containing exosomes to regulate the function of target cells. As such, exosomes are becoming seen as a new therapeutic target and biomarker for various disorders, including cardiac disease.[13,14]

Macrophages play a dual role as a key inflammatory component of cardiac injury and a central regulator in injury and repair.[15,16] Previous studies by us and other groups revealed that the cross-talks between macrophages and cardiac fibroblasts promote cardiac remodeling.[17,18] Infiltrated macrophages affect the function of fibroblasts through the paracrine activity of various cytokines. Thus, macrophages secrete transforming growth factor-β (TGF-β) and interleukin-6 (IL-6) to regulate the proliferation and activation of fibroblasts.[15,19] Macrophages can also transfer beta-glucuronidase into fibroblasts to improve the fibroblast enzymatic activity.[20] However, it remains unknown whether exosomes can mediate cross-talk between macrophages and fibroblasts.

In this study, we showed that mir-155 expression was increased in exosomes of activated macrophages. mir-155-enriched exosomes suppressed fibroblast proliferation and promoted fibroblast inflammation. mir-155 deficiency significantly decreased the incidence of cardiac rupture and improved cardiac function after acute myocardial infarction (AMI), while the transfusion of macrophage exosomes to mir-155$^{-/-}$ mice increased cardiac rupture.

Received 9 March 2016; accepted 26 September 2016;
http://dx.doi.org/10.1016/j.ymthe.2016.09.001.

Correspondence: Jie Du, Beijing Anzhen Hospital, Capital Medical University, Beijing 100029, China.
E-mail: jdu@bcm.edu
Correspondence: Yulin Li, Beijing Anzhen Hospital, Capital Medical University, Beijing 100029, China.
E-mail: lyllyl_1111@163.com

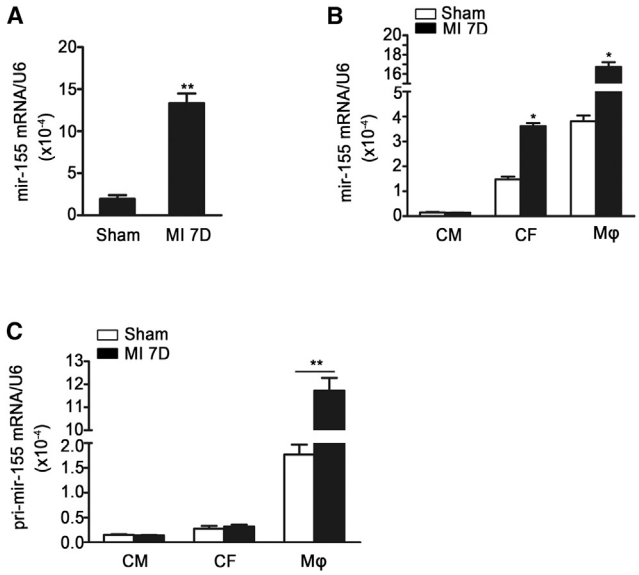

Figure 1. The mir-155 Expression Is Increased in Heart after AMI

(A) Shown is qRT-PCR analysis of mir-155 relative folds to U6 expression in the infarcted heart 7 days after myocardial infarction (MI) (n = 3 per group). Data are mean ± SEM. Paired t test was used. **p < 0.01 versus Sham operation. (B) qRT-PCR shows the mir-155 relative folds to U6 expression in cardiomyocytes (CM), cardiac fibroblasts (CF), and macrophages (Mφ) isolated from the sham-operated and infarcted hearts (n = 3 per group). Data are mean ± SEM. Paired t test was used. *p < 0.05 versus Sham. $p < 0.05 versus Sham operation. (C) Shown is the pri-mir-155 relative folds to GAPDH in cardiomyocytes (CM), cardiac fibroblasts (CF), and macrophages (Mφ) isolated from the sham-operated and infarcted hearts (n = 3 per group). Data are mean ± SEM. Paired t test was used. **p < 0.01 versus Sham operation.

RESULTS

mir-155 Expression Is Increased in the Mouse Heart after AMI

It is known that mir-155 regulates inflammation during cardiac remodeling.[21] We examined its expression and found that mir-155 expression was significantly increased in the mouse heart 7 days after AMI (Figure 1A). To determine the source of mir-155 expression in infarcted hearts, cardiomyocytes, cardiac fibroblasts, endothelial cells, and macrophages were isolated from sham and infarcted hearts. The level of mir-155 was the highest in macrophages, moderate in fibroblasts and endothelial cells, and low in cardiomyocyte after myocardial infarction. Mir-155 expression was increased in both infiltrated macrophages and cardiac fibroblasts, but the expression of pri-mir-155 was only upregulated in macrophages, suggesting that mir-155 is produced in infiltrated macrophages and is transferred into cardiac fibroblasts (Figures 1B, 1C, and S1C).

Macrophage-Derived Exosomes Transfer mir-155 into Cardiac Fibroblasts

To show the purity of isolated exosomes, electron microscopy and western blotting were performed on the exosomes from the same amount of macrophages treated with PBS, lipopolysaccharide (LPS), or AngII (Figure 2A). Electron microscopy showed the isolated exosomes which appeared as vesicles of 40–100 nm in diameter (Figure 2B). Macrophages expressed macrophage marker CD68 and organelle proteins, and exosome expressed CD68 and exosome marker Alix, but not the organelle proteins by western blot (Figure 2C). Macrophages activated by LPS or AngII secreted more exosomes than non-activated macrophages (Figure 2C). Exosomes of the same protein content were used for RNA extraction. The treatment of macrophages by LPS or AngII increased the RNA content in the same amount of exosomes (Figure 2D). To demonstrate the fibroblast uptake of exosomes, cardiac fibroblasts were cultured with exosomes from $DilC_{16}3$-labeled macrophages. As shown in Figure 2E, $DilC_{16}3$-labeled exosomes were efficiently transferred into cardiac fibroblasts. Taken together, these results show that activated macrophages secrete more exosomes than non-activated macrophages, which can be taken up by cardiac fibroblasts.

Next, we found that mir-155 expression was increased in activated macrophages, which was consistent with previous studies[22,23] (Figure 3A). When cardiac fibroblasts were co-cultured with exosomes derived from activated macrophages, the mir-155 mRNA level was markedly increased in fibroblasts (Figure 3B). To examine dose-dependent effect of exosomes on fibroblasts, dose-response curve experiments were performed. With the increase doses of exosome, the mir-155 expression in fibroblasts was increased (Figure S2B). However, pri-mir-155 level was unchanged, indicating that the increase of mir-155 in cardiac fibroblasts was not caused by the fibroblasts themselves (Figure 3C).

To further demonstrate that transfer of mir-155 from macrophages into cardiac fibroblasts is mediated by exosomes, we co-cultured fibroblasts with supernatant of cultured macrophages. We observed a significant increase in mir-155 levels in cardiac fibroblasts co-cultured with the supernatant from Ang-II-activated wild-type (WT) macrophages (Figure 3D), while mir-155 expression was unchanged in Ang-II-treated fibroblasts. Cardiac fibroblasts were then separately co-cultured with macrophage supernatant or exosome-depleted macrophage supernatant. The level of mir-155 was low when exosomes were removed from the supernatant (Figure 3E), indicating that the mir-155 elevation was caused by the presence of the exosomes. We subsequently confirmed this observation using mir-$155^{-/-}$ cardiac fibroblasts co-cultured with exosomes isolated from WT or mir-$155^{-/-}$ macrophages stimulated by PBS or AngII. qRT-PCR showed that mir-155 expression increased in mir-$155^{-/-}$ cardiac fibroblasts after the addition of exosomes secreted from AngII-stimulated WT macrophages (Figure 3F). These results demonstrate that the fibroblasts themselves do not express mir-155, and that macrophage-derived exosomes transfer mir-155 into cardiac fibroblasts.

mir-155-Containing Macrophage Exosomes Suppress Cardiac Fibroblast Proliferation by Inhibiting Son of Sevenless Expression

To evaluate the role of exosome-contained mir-155 after transfer into cardiac fibroblasts, the TargetScan (v.7.1) was used to predict the target genes of mir-155, and 427 genes from mouse and 674 genes from human were founded. 349 common genes for both human

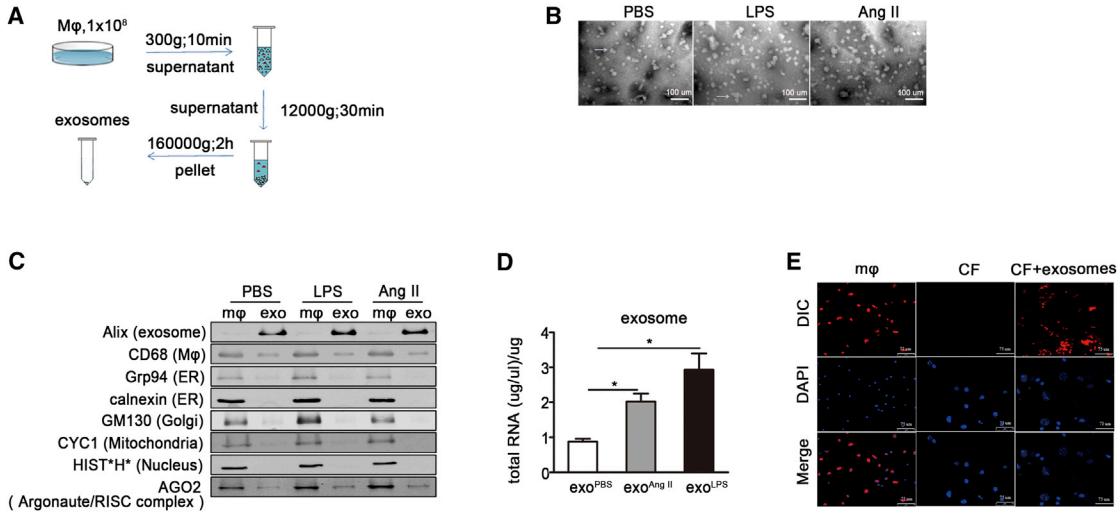

Figure 2. Activated Macrophages Secrete Exosomes that Are Taken up by Cardiac Fibroblasts

(A) Flow chart depicts the differential centrifugation protocol. Macrophages were first stimulated by lipopolysaccharide (LPS) or Ang II for 24 hr. Exosomes were then collected by differential centrifugation. (B) Shown are the representative Electron microscopy pictures for exosomes isolated from macrophage stimulated by PBS, LPS, or AngII. Scale bar, 1 nm. (C) Representative western blotting shows the exosome marker Alix, macrophage marker CD68, Endoplasmic reticulum (ER) marker Grp94 and calnexin, Golgi marker GM130, Mitochondria marker cytochrome *c* (CYC1), Nucleus marker histones (HIST*H*), and Argonaute/RISC complex marker AGO on macrophages and exosomes isolated from macrophage stimulated by PBS, LPS, or AngII. (D) RNA content of the same protein amount of exosomes derived from macrophage stimulated with PBS, LPS, or AngII (n = 3 per group). *$p < 0.05$ versus exosome derived from PBS-treated macrophage. (E) Shown are confocal images of macrophages stained with $DiIC_{16}3$, a phospholipid membrane dye (top), and cardiac fibroblasts after incubation with exosomes from stained macrophage for 48 hr (bottom). Scale bar, 10 μm.

and mouse were selected and used them for gene ontology pathway analysis. As shown in Figure 4A, the main effect of mir-155 include roles in cancer pathways, B- and T cell receptor signaling, the neurotrophin signaling, the MAPK signaling, and the cell-cycle signaling. We focused on the cell cycle as fibroblast proliferation is a key event that occurs during cardiac injury and repair. We first assessed the proliferation capacity of cardiac fibroblasts in response to mir-155. Bromodeoxyuridine (BrdU) staining showed that a mir-155 mimic suppressed the Ang-II-induced proliferation of cardiac fibroblasts (Figure 4B). Importantly, in contrast to exosomes from PBS-stimulated macrophages, exosomes from AngII-stimulated WT macrophages, but not AngII-stimulated mir-155$^{-/-}$ macrophages, inhibited the proliferation of fibroblasts (Figure 4C). Dose-response curve experiment also showed a dose-dependent inhibition of the fibroblasts proliferation (Figure S4A). To further confirm the role of mir-155 in fibroblast proliferation, WT fibroblasts were incubated with WT exosomes in the presence of a mir-155 inhibitor. BrdU staining showed that the mir-155 inhibitor rescued the reduced proliferation of fibroblasts induced by WT exosomes (Figure 4D). Together, these results show that mir-155-containing macrophage exosomes suppress cardiac fibroblast proliferation.

To ascertain the mechanism by which mir-155 affects cardiac fibroblasts, we analyzed the predicted target genes of mir-155 involved in cell proliferation. The Son of Sevenless gene (*Sos1*) contains two predicted mir-155 target sequences in its 3′ UTR (Figure 4E). Sos1 is the main mediator of Ras activation and is critical to cell proliferation through its activation of the Ras-GTP state and ERK phosphorylation.[24,25] Luciferase reporter assays showed that the mir-155 mimic reduced the activity of the reporter plasmid containing a 3′-UTR sequence of Sos1. We searched two mir-155 binding sites on Sos1 by TargetScan. The plasmids with the mutation on each binding site and on both binding sites were constructed to carry out the luciferase reporter assay. The results showed that the decrease in Sos1 expression was abolished when Sos1 binding sites were mutated (Figure 4F). Moreover, western blotting revealed that the mir-155 mimic suppressed Sos1 protein expression in cardiac fibroblasts (Figure 4G). Sos1 expression was shown by qRT-PCR to be increased in cardiac fibroblasts after Ang II stimulation (Figure 4H), while Sos1 small inhibiting small interfering RNA (siRNA) decreased Sos1 expression by 57% (Figure 4I). Finally, *Sos1* knockdown in cardiac fibroblasts significantly reduced their cellular proliferation, as revealed by BrdU staining (Figure 4J). To further demonstrate that mir-155 inhibits fibroblast proliferation by decreasing Sos1 expression, mir-155$^{-/-}$ fibroblasts were co-cultured with exosomes from AngII-treated wild-type macrophages (exo$^{\text{AngII-WT Mφ}}$) for 48 hr and examined for BrdU incorporation. exo$^{\text{AngII-WT Mφ}}$ inhibited Sos1 expression and fibroblasts proliferation, and treatment mir-155$^{-/-}$ fibroblasts with Sos1 siRNA decreased fibroblast proliferation (Figures S3B and S3C). Together, these results demonstrate that mir-155-containing exosomes suppress cardiac fibroblast proliferation by downregulating Sos1 expression.

mir-155-Containing Macrophage Exosomes Promote Inflammation in Cardiac Fibroblasts

Because mir-155 has a known inflammatory function, we evaluated the role of mir-155-containing exosomes on the inflammation of

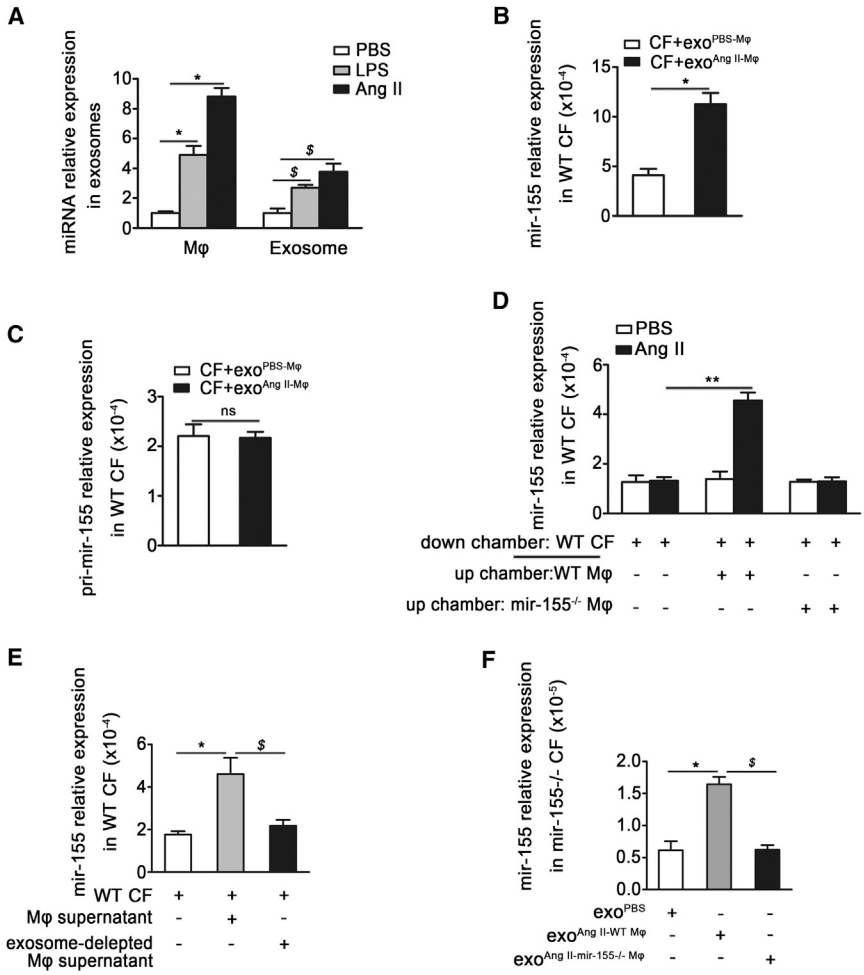

Figure 3. Macrophage-Secreted mir-155 Can Be Transferred into Cardiac Fibroblasts

(A) qRT-PCR shows the relative folds of mir-155 to U6 expression in macrophage and macrophage-secreted exosomes stimulated with LPS or Ang II (n = 3 per group). Data are mean ± SEM. Paired t test was used. *p < 0.05 versus PBS. $p < 0.05 versus exosome isolated from PBS-treated macrophages. (B) The mir-155 relative folds to U6 expression in 1 × 10^5 cardiac fibroblasts co-cultured with exosomes (40 μg/ml) isolated from PBS or Ang-II-stimulated macrophages (n = 3 per group). Data are mean ± SEM. Paired t test was used. *p < 0.05 versus CF+exo$^{PBS\text{-}M\varphi}$. (C) The relative folds of pri-mir-155 expression to GAPDH in cardiac fibroblasts co-cultured with exosomes isolated from PBS or Ang-II-stimulated macrophages (n = 3 per group). Data are mean ± SEM. Paired t test was used. *p < 0.05 versus CF+exo$^{PBS\text{-}M\varphi}$. (D) mir-155 relative folds to U6 expression are detected by qRT-PCR in WT cardiac fibroblasts co-cultured with the supernatant of AngII-stimulated WT macrophages and the supernatant of AngII-stimulated mir-155 deficiency (mir-$155^{-/-}$) macrophages that were stimulated by Ang II for 48 hr (n = 3 per group). Data are mean ± SEM. Paired t test was used. **p < 0.01 versus Ang II. (E) qRT-PCR shows the mir-155 relative folds to U6 expression in WT cardiac fibroblasts co-cultured with the supernatant of WT macrophage stimulated by Ang II for 24 hr or exosome-depleted macrophage supernatant (n = 3 per group). Data are mean ± SEM. Paired t test was used. *p < 0.05 versus basal medium. $p < 0.05 versus Mφ supernatant. (F) qRT-PCR analysis of mir-155 relative folds to U6 expression in mir-$155^{-/-}$ cardiac fibroblasts after respectively incubation with exosomes from PBS or Ang-II-stimulated WT macrophages or exosomes from Ang-II-stimulated mir-$155^{-/-}$ macrophages (n = 3 per group). Data are mean ± SEM. Paired t test was used. *p < 0.05 versus exo$^{PBS\text{-}WT\ M\varphi}$. $p < 0.05 versus exo$^{Ang\ II\text{-}WT\ M\varphi}$.

cardiac fibroblasts. Using qRT-PCR and the cytometric bead array, we found that inflammatory cytokines IL-1β, IL-6, tumor necrosis factor alpha (TNF-α), and chemokine (C-C motif) ligand (CCL)-2 were significantly increased in fibroblasts transfected with the mir-155 mimic compared with those transfected with the control mimic (Figures 5A and 5B). The anti-inflammatory gene Suppressor of Cytokine Signaling 1 (*Socs1*) has previously been reported to be a target of mir-155.[26] We found that the mir-155 mimic decreased Socs1 protein expression in cardiac fibroblasts, which was associated with increased Stat3 phosphorylation (Figure 5C). To further confirm whether exosome-containing mir-155 has the same effect on fibroblast inflammation, we incubated cardiac fibroblasts with WT exosomes upon exposure to a mir-155 inhibitor. Similarly, macrophage-derived exosomes increased the expression of inflammatory cytokines IL-1β, IL-6, TNF-α, and CCL-2 at both the mRNA and protein level. Importantly, the mir-155 inhibitor blocked the pro-inflammatory response induced by macrophage-derived exosomes (Figures 5D and 5E). The pro-inflammatory role of exosomes showed a dose-dependence that is the fibroblasts inflammation was increased with the increase of exosome (Figure S4A). In order to demonstrate that mir-155 increases fibroblast inflammation by decreasing Socs1 expression, mir-$155^{-/-}$ fibroblasts were cocultured with exo$^{AngII\text{-}WT\ M\varphi}$ for 48 hr, and the mRNA level of inflammatory cytokines was examined. exo$^{AngII\text{-}WT\ M\varphi}$ inhibited Socs1 expression and enhanced inflammation, and knockdown of Socs1 in mir-$155^{-/-}$ fibroblasts increased the fibroblast inflammation (Figures S4B and S4C). Together, these data suggest that macrophages promote an inflammatory response in cardiac fibroblasts by transferring mir-155-containing exosomes.

mir-155 Deficiency Reduces the Incidence of Cardiac Rupture after AMI

Fibroblast proliferation and inflammation play an important role in cardiac repair after AMI.[27] We next evaluated the effect of mir-155 on AMI in vivo. We observed a significantly higher survival rate ≤7 days after AMI in mir-$155^{-/-}$ compared with WT mice (68% versus 50% in the respective genotypes; Figure 6A). Cardiac rupture was also more prevalent in WT mice than mir-$155^{-/-}$ mice (Figure 6B). Moreover, immunohistochemical staining and Masson trichrome staining showed that mir-$155^{-/-}$ mice possessed a higher

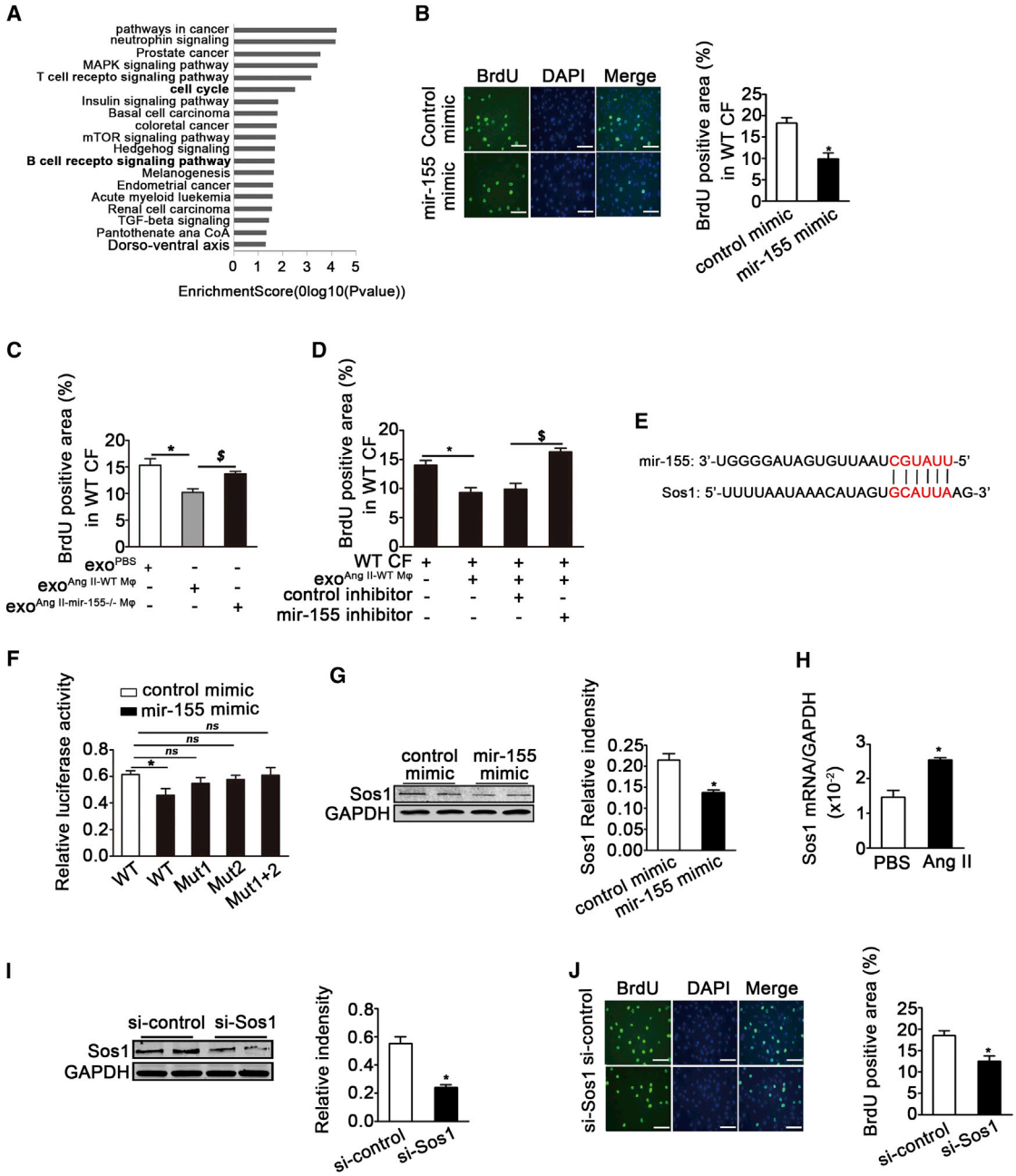

Figure 4. mir-155-Containing Macrophage Exosomes Suppress the Proliferation of Recipient Cardiac Fibroblasts by Downregulating Sos1 Protein

(A) Go and Pathway analysis were performed on mir-155 target genes predicted by TargetScan base. (B) Shown is the BrdU staining and quantification of BrdU positive cells of cardiac fibroblasts treated with mir-155 mimic or control mimic RNAs for 48 hr (n = 3 per group). *p < 0.05 versus control mimic. Scale bar, 100 nm. (C) Shown is quantification of BrdU staining of cardiac fibroblasts treated with exosomes isolated from PBS or Ang-II-stimulated WT macrophages or exosomes from Ang-II-stimulated mir-155$^{-/-}$ macrophages (n = 3 per group). *p < 0.05 versus exo$^{PBS\text{-}WT\ M\varphi}$. $^{\$}$p < 0.05 versus exo$^{Ang\ II\text{-}M\varphi}$. (D) Shown is BrdU staining of WT exosomes-treated cardiac fibroblasts transfected with control inhibitor or mir-155 inhibitor (n = 3 per group). *p < 0.05 versus PBS. $^{\$}$p < 0.05 versus fibroblast treated with exo$^{Ang\ II\text{-}M\varphi}$ and control inhibitor. (E) The predicted mir-155 seed sequence in the Sos1 3′-UTR region is shown. (F) The graph shows the effect of mir-155 on wild-type and mutated Sos1 luciferase reporter assay (n = 3 per group). *p < 0.05 versus control mimic. (G) Western blotting analysis and quantification of Sos1 protein level in lysates of cardiac fibroblasts transfected with mir-155 mimic or control mimic RNAs (n = 3 per group). *p < 0.05 versus control mimic. (H) qRT-PCR analysis of Sos1 relative folds to GAPDH in cardiac fibroblasts stimulated with PBS or Ang II is shown (n = 3 per group). Data are mean ± SEM. Paired t test was used. *p < 0.05 versus PBS. (I) Western blotting analysis and quantification of Sos1 protein level of cardiac fibroblasts transfected with si-control or si-Sos1 (n = 3 per group). *p < 0.05 versus si-control. (J) Representative images of BrdU positive cells of cardiac fibroblasts transfected with si-control or si-Sos1 (right panel). Bar graph shows quantification of BrdU positive cells (left panel) (n = 3 per group). *p < 0.05 versus si-control. Scale bar, 100 nm.

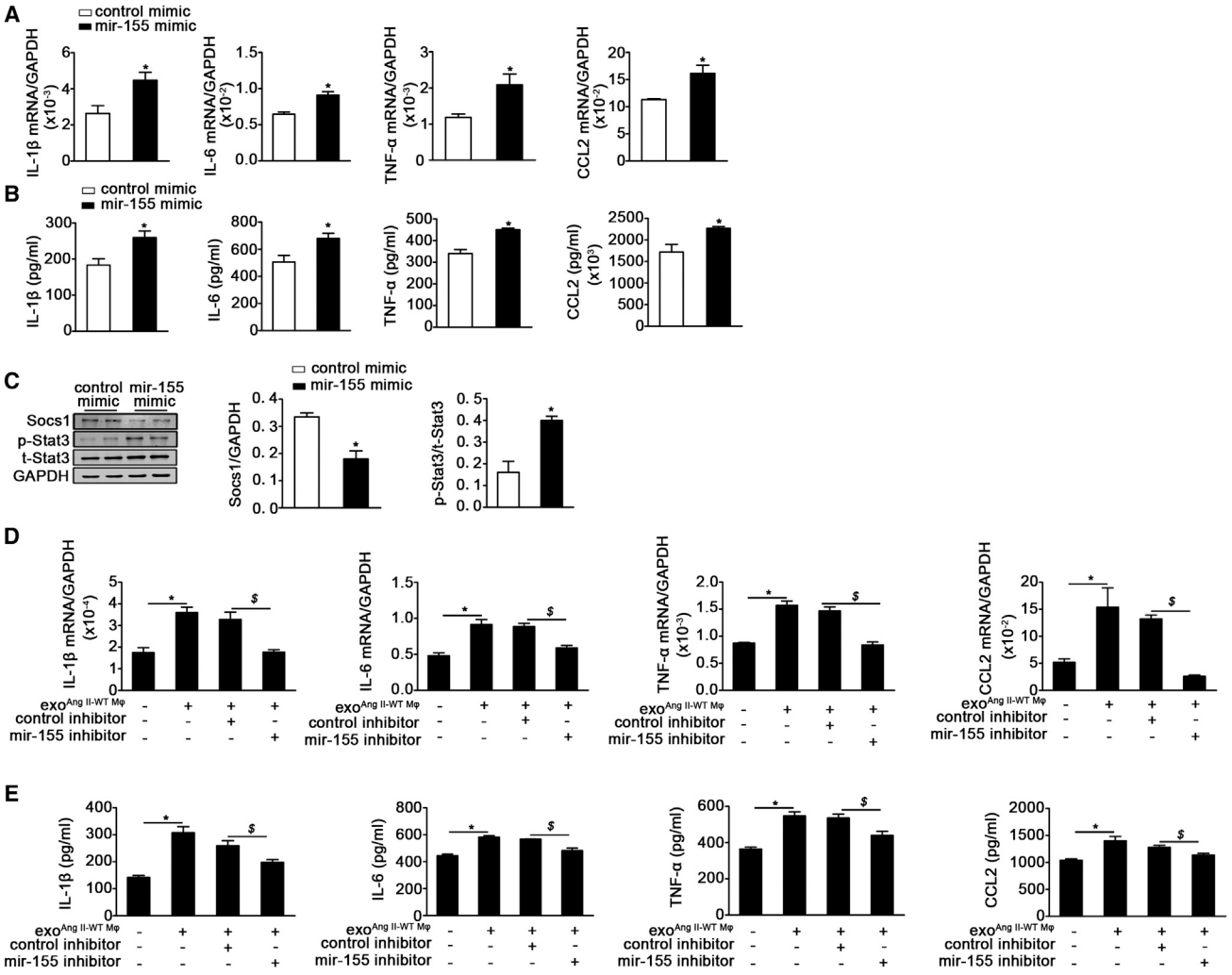

Figure 5. mir-155-Containing Macrophage Exosome Aggravates Fibroblasts Inflammation by Regulation of Socs1/Stat3 Signaling

(A and B) Respectively showed the mRNA (A) and protein (B) level of IL-1β, IL-6, TNF-α, and CCL2 expression in cardiac fibroblasts transfected with control mimic or mir-155 mimic (n = 3 per group). Data are mean ± SEM. Paired t test was used. *$p < 0.05$ versus control mimic. (C) Representative western blotting images and quantification of Socs1, phosphorylated Stat3 (p-Stat3), and total Stat3 (t-Stat3) in cardiac fibroblasts transfected with control mimic or mir-155 mimic (n = 3 per group). *$p < 0.05$ versus control mimic. (D and E) Shown are the mRNA and protein level of IL-1β, IL-6, TNF-α, and CCL2 in WT exosomes-treated cardiac fibroblasts with or without mir-155 inhibitor (n = 3 per group). Data are mean ± SEM. Paired t test was used. *$p < 0.05$ versus PBS. $^{\$}p < 0.05$ versus fibroblast treated with $exo^{Ang\ II\text{-}M\varphi}$ and control inhibitor.

number of collagen I-positive and α-smooth muscle actin (SMA)-positive cells and a higher degree of collagen disposition in the infarcted area of the heart compared with WT mice 7 days after AMI (Figures 6C and 6D). Similarly, qRT-PCR also revealed the increased mRNA expression of α-smooth muscle actin, collagen I, and collagen III in the infarcted area of mir-155$^{-/-}$ mice (Figure 6E).

The measurement of cardiac function by echocardiography revealed an alleviated cardiac dilatation and an ameliorative LV function in mir-155$^{-/-}$ mice compared with WT mice (Figure 6F). To further clarify the effect of mir-155-containing macrophage exosomes on cardiac repair, we carried out a transfusion of AngII-stimulated WT macrophage-secreted exosomes into mir-155$^{-/-}$ mice. The two doses of exosomes (100 or 200 μg) were first injected 30 min before the operation, three injections were performed at days 2, 4, or 6 after myocardial infarction, and the effect of exosome on the prognosis of myocardial infarction was examined (Figure 6G). The results showed that the mir-155 expression was increased in heart, the mortality rate was higher, and the collagen deposition in the infarct border area was decreased when the dose of exosome increased. Moreover, injection of exosomes from AngII-stimulated WT macrophages exhibited an increased expression of mir-155, increased cardiac rupture rate, and a decreased collagen deposition in heart compared to injection of exosomes from AngII-stimulated mir-155$^{-/-}$ macrophages to miR-155$^{-/-}$ recipients (Figures 6H–6J). Taken together, these data indicate that the mir-155 deficiency suppressed the cardiac rupture

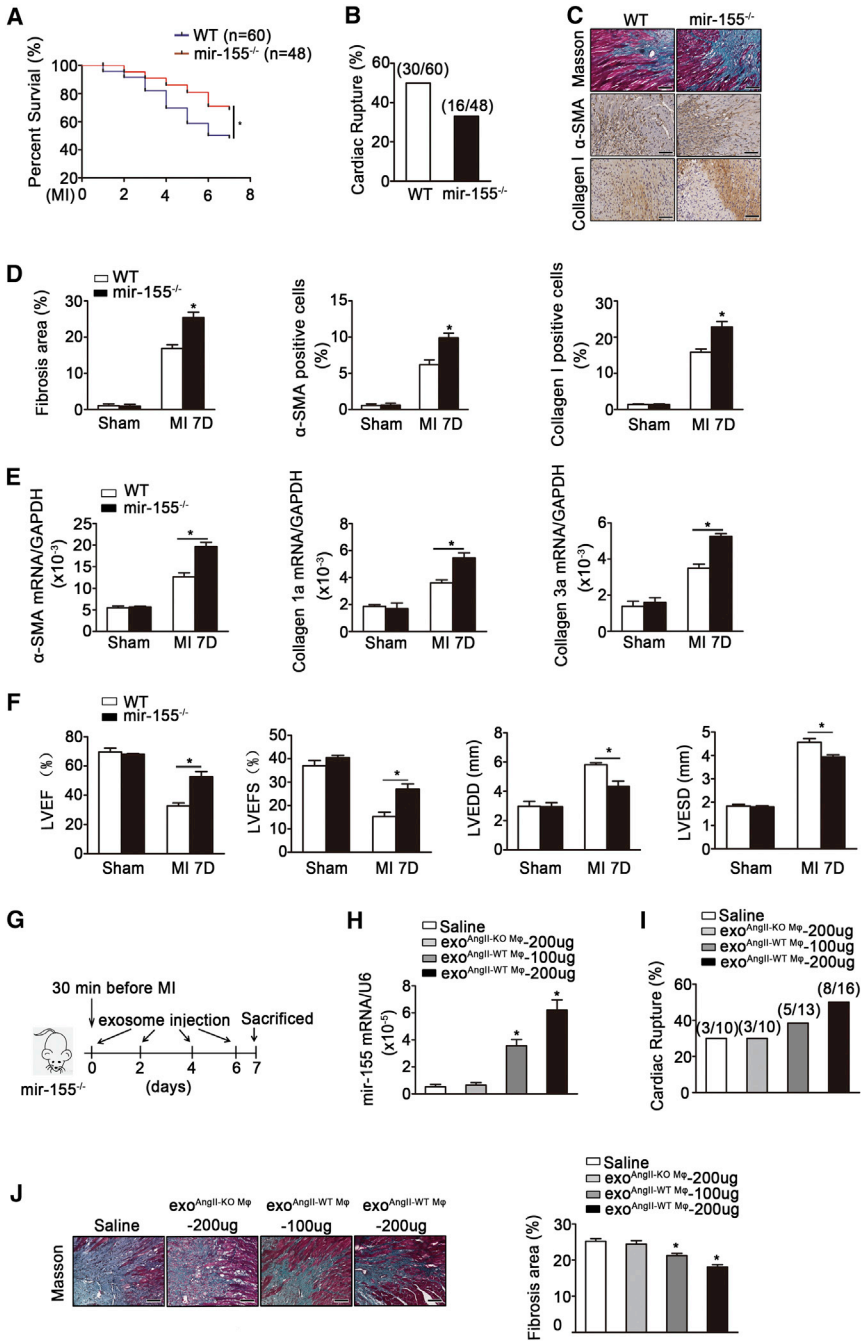

Figure 6. mir-155 and mir-155-Containing Exosomes Led to Cardiac Rupture and Adverse Prognosis of Myocardial Infarction

(A) Survival curves of WT mice and mir-155$^{-/-}$ mice after AMI (n = 60 for WT mice and n = 48 for mir-155$^{-/-}$ mice) *p < 0.05 versus WT. (B) Prevalence of death caused by cardiac rupture after AMI (n = 60 for WT mice and n = 48 for mir-155$^{-/-}$ mice). (C) Representative Masson trichrome staining and immunohistochemical staining of Collagen I and α-SMA on infarcted area of WT and mir-155$^{-/-}$ heart tissue 7 days after AMI (n = 9 per group). Scale bar, 100 nm. (D) Quantification of fibrosis, the ratio of α-SMA positive staining and Collagen I positive staining to total myocardial tissue (n = 9 per group). *p < 0.05 versus WT mice after MI. (E) qRT-PCR showed the relative folds of α-SMA, Collagen I, and Collagen III to GAPDH on infarcted heart of WT and mir-155$^{-/-}$ mice (n = 9 for WT mice and n = 11 for mir-155$^{-/-}$ mice). Data are mean ± SEM. Paired t test was used. *p < 0.05 versus WT Sham. $^{\$}$p < 0.05 versus WT mice after MI. (F) Shown are LVEF, LVFS, LVEDD, and LVESD of WT and mir-155$^{-/-}$ mice 7 days after AMI by echocardiography analysis. *p < 0.05 versus WT mice after MI. (G) Flow chart depicting the transfusion experiment design. (H) Shown is the mir-155 relative folds to U6 expression in the heart of mir-155$^{-/-}$ mice transfused with saline, mir-155$^{-/-}$ Mφ-secreted exosomes (200 μg) and WT Mφ-secreted exosomes (100 or 200 μg) (n = 3 for mir-155$^{-/-}$ mice transfected with saline or exo$^{KO\ M\varphi}$-200 μg, n = 4 for mir-155$^{-/-}$ transfected with exo^{WT} Mφ). *p < 0.05 versus mir-155$^{-/-}$ mice transfected with exo$^{KO\ M\varphi}$-200 μg. (I) Prevalence of death because of cardiac rupture after acute myocardial infarction in mir-155$^{-/-}$ mice transfused with saline, mir-155$^{-/-}$ Mφ-secreted exosomes (200 μg), or WT Mφ-secreted exosomes (100 or 200 μg). (J) Shown is Masson trichrome staining and quantification of fibrosis on infarcted area of saline, mir-155$^{-/-}$ Mφ-secreted exosomes (200 μg) or WT Mφ-secreted exosomes (100 or 200 μg) transfused heart tissue 7 days after AMI (n = 3 for mir-155$^{-/-}$ mice transfected with saline or exo$^{KO\ M\varphi}$-200 μg, n = 4 for mir-155$^{-/-}$ transfected with exo^{WT} Mφ). Data are mean ± SEM. Paired t test was used. *p < 0.05 versus mir-155$^{-/-}$ mice transfected with exo$^{KO\ M\varphi}$-200 μg. Scale bar, 100 nm.

and dysfunction of myocardial infarction, and that this cardiac protection could be abolished in mir-155$^{-/-}$ mice transfused by macrophage-derived exosome.

mir-155 Deficiency Accelerated Cardiac Fibroblast Proliferation and Alleviated Inflammation after AMI

We evaluated the role of mir-155 in cardiac fibroblast proliferation and inflammation in vivo. mir-155 deficiency increased Sos1 expression (western blotting) and fibroblast proliferation (BrdU staining) in infarcted hearts (Figures 7A and 7B). Socs1 (another target gene of mi-155) expression was also increased (Figure 7C). H&E staining showed a decreased inflammation and a reduced infiltration of macrophages in the infarcted area of the mir-155$^{-/-}$ heart (Figure 7D). We also found significant reductions in the mRNA levels of IL-1β, IL-6, TNF-α, and CCL2 in mir-155$^{-/-}$ mouse hearts compared with those of WT mice 7 days after myocardial infarction (Figure 7E).

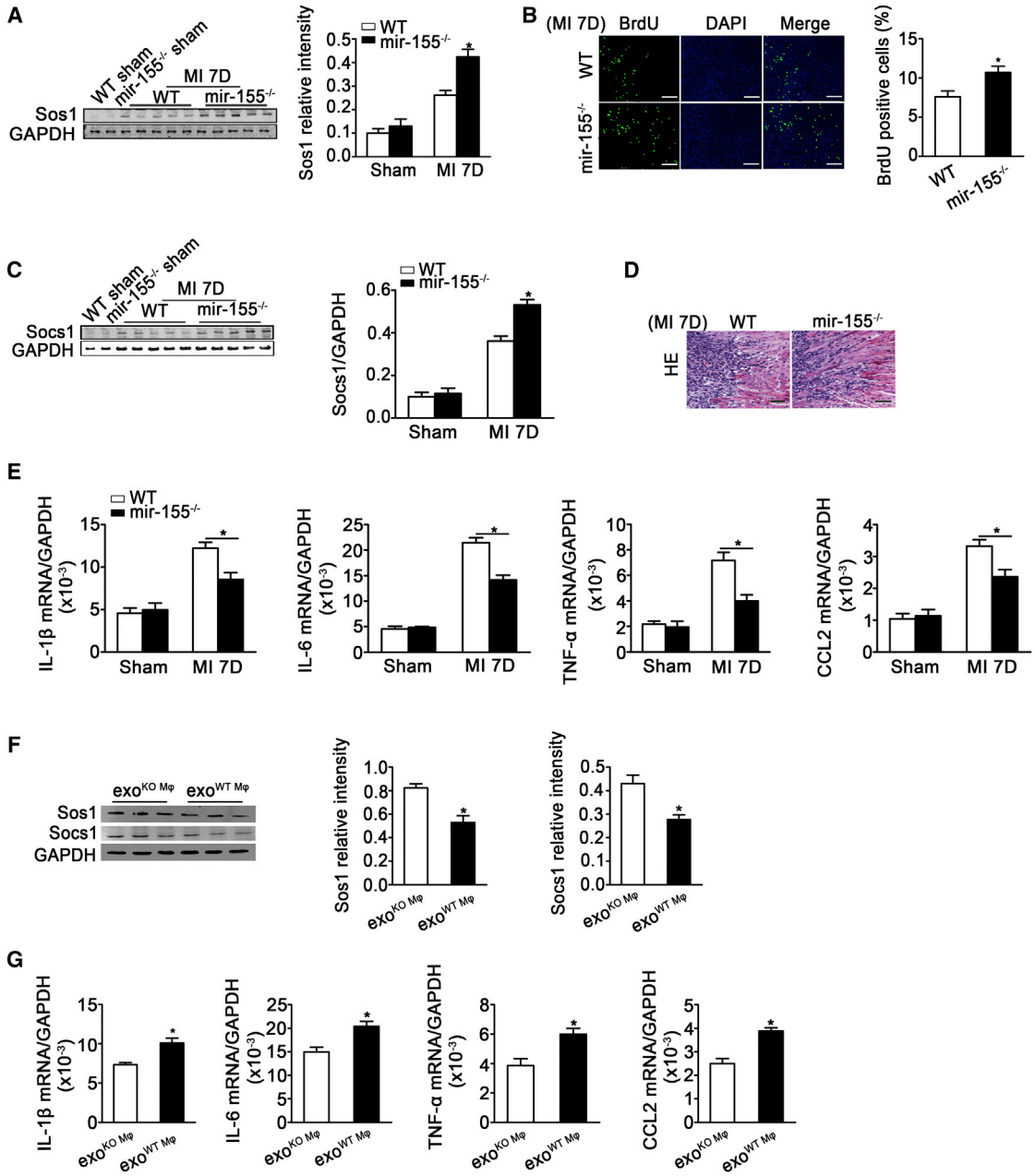

Figure 7. mir-155 Deficiency Increases Fibroblasts Proliferation and Decreases Inflammation

(A) Western blotting analysis and quantification of Sos1 expression in the heart of infarcted WT and mir-155$^{-/-}$ mice (n = 9 per group). *p < 0.05 versus WT mice after MI. (B) Shown is BrdU staining and quantification of BrdU positive cells of proliferative cells in infarcted heart (n = 3 per group). *p < 0.05 versus WT mice after MI. Scale bar, 100 nm. (C) Western blotting analysis and quantification of Socs1 expression in the heart of infarcted WT and mir-155$^{-/-}$ mice (n = 9 per group). *p < 0.05 versus WT mice after MI. (D) Shown are H&E staining on the infarcted area of WT and mir-155$^{-/-}$ heart tissue 7 days after AMI (n = 9 per group). Scale bar, 100 nm. (E) Real-time PCR analysis of IL-1β, IL-6, TNF-α, and CCL-2 mRNA levels in WT and mir-155$^{-/-}$ mouse hearts (n = 9 for WT mice and n = 11 for mir-155$^{-/-}$ mice). Data are mean ± SEM. Paired t test was used. *p < 0.05 versus WT mice after MI. (F) Western blotting analysis and quantification of Sos1 and Socs1 expression in the heart of mir-155$^{-/-}$ mice transfused with AngII-stimulated mir-155$^{-/-}$ Mφ-secreted exosomes (exo$^{\text{AngII-KO Mφ}}$) or AngII-stimulated WT Mφ-secreted exosomes (exo$^{\text{AngII-WT Mφ}}$). n = 3 per group. *p < 0.05 versus exo$^{\text{AngII-KO Mφ}}$. (G) Shown is the IL-1β, IL-6, TNF-α, and CCL2 relative folds to GAPDH expression in the heart of mir-155$^{-/-}$ mice transfused with AngII-stimulated mir-155$^{-/-}$ Mφ-secreted exosomes (exo$^{\text{AngII-KO Mφ}}$) or AngII-stimulated WT Mφ-secreted exosomes (exo$^{\text{AngII-WT Mφ}}$) (n = 3 per group). Data are mean ± SEM. Paired t test was used. *p < 0.05 versus exo$^{\text{AngII-KO Mφ}}$.

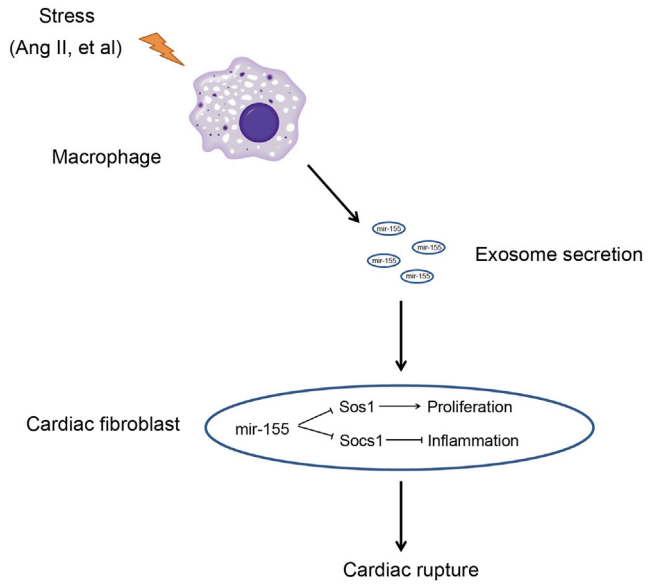

Figure 8. Summarize the Role of mir-155-Containing Mφ Exosomes on Cardiac Fibroblasts Proliferation and Inflammation

During cardiac injury, activated macrophages secrete mir-155-enriched exosomes that are transported into cardiac fibroblasts. Macrophage-derived mir-155 suppresses proliferation and promotes inflammation of fibroblast, which leads to cardiac rupture after AMI.

We examined the expression of Sos1 and Socs1 and inflammation in mir-155$^{-/-}$ mice transfused with exosomes from AngII-stimulated WT macrophages (exo$^{\text{AngII-WT Mφ}}$) or exosomes from AngII-stimulated mir-155$^{-/-}$ macrophages (exo$^{\text{AngII-KO Mφ}}$). The results showed that mir-155$^{-/-}$ mice transfused with exo$^{\text{AngII-WT Mφ}}$ had an increased inflammation and a decreased Sos1 and Socs1 expression in heart (Figures 7F and 7G). Taken together, these results show that mir-155$^{-/-}$ increases cardiac fibroblast proliferation and decreases inflammation.

DISCUSSION

In this study, we demonstrated that activated macrophages secrete mir-155-containing exosomes, and that these exosomes can be taken up by cardiac fibroblasts. The mir-155 mimic or mir-155-containing macrophage exosomes suppressed fibroblast proliferation by downregulating Sos1 protein expression and increasing fibroblast inflammation by decreasing Socs1 expression. The mir-155 deficiency ameliorated cardiac rupture and eventually improved cardiac function in response to myocardial infarction. Moreover, the transfusion of macrophage exosomes into mir-155$^{-/-}$ mice exacerbated cardiac rupture. These results demonstrate that mir-155-containing exosomes play an important role in the crosstalk between fibroblasts and macrophages, as well as in cardiac repair after AMI (summarized in Figure 8).

Macrophages contain abundant mir-155,[28] and its level was markedly upregulated in LPS- and Ang-II-treated macrophages (Figure 3). Previously, miRNAs were reported to be selectively packaged into exosomes in response to different stimuli.[11] This selective packaging is partly caused by the elevation of specific miRNA expression in donor cells. Along with these observations, we found that mir-155 expression was significantly elevated in response to Ang II, which possibly leads to the active packaging of mir-155 into exosomes.

We found that macrophage-secreted exosomes were taken up by cardiac fibroblasts and mediated macrophage-fibroblast crosstalk. In vitro, exosomes or conditioned medium from activated macrophages, but not exosome-deleted conditioned medium, upregulated the mir-155 expression in cardiac fibroblasts. However, there was no change to mir-155 expression in cardiac fibroblasts under stimulation. A recent in vivo study showed that AMI significantly upregulated the expression of mir-155 in cardiac fibroblasts.[29] In the present study, we showed that the expression of pri-mir-155 was unchanged in cardiac fibroblasts after AMI (Figure 1), demonstrating that the increase of mir-155 in fibroblasts occurs as a result of macrophage-secreted exosome delivery.

The biological role of exosomes on target cells is dependent on the selectively packaged miRNA content. Although the mir-155 is well studied in macrophages for its function in inflammation and macrophage differentiation,[30] its role in cardiac fibroblasts is largely unknown. In this study, we found that mir-155-containing exosomes have an important effect on cardiac fibroblasts, based on the following results: (1) the mir-155 mimic directly suppressed proliferation and promoted inflammation in cardiac fibroblasts; (2) macrophage-derived exosomes play a similar role in fibroblasts; and (3) exosome-mediated anti-proliferation and proinflammation in cardiac fibroblasts was blocked by the addition of a mir-155 inhibitor.

We report that Sos1, as a new target gene of mir-155, is involved in mir155-containing exosome-mediated anti-proliferation in cardiac fibroblasts. Sos1 is a dual guanine nucleotide exchange factor that binds to Ras, which is important in regulating cell growth.[31] Sos1 promotes cell proliferation by enhancing ERK activity through increasing the Grb2-Sos1 complex formation.[25] We showed that mir-155 downregulated Sos1 protein levels in cardiac fibroblasts, that Sos1 expression was increased in proliferative cardiac fibroblasts, and that knockdown of Sos1 significantly inhibited cardiac fibroblast proliferation (Figure 4). It is known that AT-1R is also a target of mir155,[32] thus our new finding that Sos1, an intracellular target of mir-155, added new molecules in regulating fibroblast function. Socs1 has previously been shown to be a target of mir-155 involved in the regulation of inflammation.[21] It is an inflammation suppressor that normally functions as a negative feedback regulator of Janus activated kinase or signal transducer and activator of transcription signaling.[33] There are several reports that cardiac fibroblasts could be an inflammatory "factories,"[34,35] we also showed that cardiac fibroblasts secrete TNF-a, IL-1β, and CCL2 under inflammatory stimulation.[36] Our results show that miR-155 overexpression in cardiac fibroblasts promoted the inflammatory response by repressing Socs1 expression. It has been shown that mir-155 inhibits the production of MMP-1 and

MMP3.[37] Thus, our finding that mir-155 regulates the phenotype of cardiac fibroblasts could be potentially mediated by regulating MMP1 and MMP3 in myocardial infarction. This possibility should be determined in the future study.

During myocardial infarction, cardiac fibroblasts mainly proliferate, deposit collagen, and secrete cytokines. In the early phase of myocardial infarction, cardiac fibroblast proliferation prevents cardiac rupture, improves the survival rate, and promotes cardiac repair.[38,39] Growing evidence shows that expansion of the inflammatory response results in cardiomyocyte death, deterioration in remodeling, and dysfunction after myocardial infarction through the release of reactive oxygen species, matrix metalloproteinase, and pro-inflammatory cytokines,[40] In this study, we demonstrate that a mir-155 deficiency increased fibroblast proliferation and collagen synthesis and reduced the inflammatory response, which would likely decrease the incidence of cardiac rupture in the early stage of myocardial infarction and improve cardiac function. Importantly, the transfusion of macrophage-derived exosomes to mir-155$^{-/-}$ mice recovered mir-155 expression in the heart and increased the incidence of cardiac rupture (Figure 6). Thus, macrophage-derived exosomes appear to impair cardiac repair after AMI at least partially through the role of mir-155.

In conclusion, we demonstrate a novel function of mir-155 in non-inflammatory cells. We showed that mir-155-containing exosomes mediate macrophage-fibroblast cross-talk. Moreover, mir-155 suppressed fibroblast proliferation and increased fibroblast inflammation, which led to an impaired cardiac repair after myocardial infarction.

MATERIALS AND METHODS

Reagents and Antibodies

Macrophage colony-stimulating factor was purchased from Pepro Tech. The following antibodies were used: anti-Alix, anti-CD68 and anti-α-smooth muscle actin (α-SMA) (Abcam), anti-Grp94, anti-calnexin, anti-GM130, anti-CYC1, anti-HIST*H*, anti-AGO2, anti-Sos1 (Cell Signaling Technology) and anti-Socs1 (Cell Signaling Technology). Anti-BrdU, anti-CD45, anti-CD11b, anti-PDGFR1, and anti-CD31 antibodies were all bought from BD (BD Biosciences). microON mir-155 mimic, microON mir-155 inhibitor and control RNAs were from GUANGZHOU RIBOBIO. si-control and si-Sos1 were purchased from Santa Cruz Biotechnology. DilC_{16}3 was from Life Technologies. Collagenase II and dispase II were obtained from Sigma-Aldrich.

Cell Culture and Reagents

Bone-marrow-derived macrophages were isolated from the femurs and tibias of adult mice as described previously.[41] Macrophages were cultured in DMEM complete medium (10% FBS and 1% penicillin and streptomycin) supplemented with murine macrophage colony-stimulating factor (50 ng/mL) at 37°C for 5 days. For cardiac fibroblasts separation, the enzymatic digestion was used as described previously.[37] Fibroblasts were cultured in DMEM complete medium at 37°C. All fibroblasts were cultured with FBS-free DMEM medium for 24 hr before experiment.

Exosome Isolation

Exosomes were isolated from conditioned medium of macrophages cultured in basal medium with or without LPS (100 ng/ml) and Ang II (1 μM) stimulation for 24 hr. Exosomes were collected by differential centrifugation. Briefly, the supernatant was centrifuged as follows: 300 × *g* for 10 min, 10,000 × *g* for 30 min, and 100,000 × *g* for 70 min (all the steps were performed at 4°C). For exosomes purification, MV pellets were followed by an additional washing step with PBS at 160,000 × *g* for 1 hr. Exosomes were re-suspended in basal medium.

Exosomes Labeling and Confocal Microscopy

Macrophages were labeled with a phospholipid membrane dye, lipophilic carbocyanine DilC_{16}3 (D384, 1.25 μM) at 37°C for 20 min.[12] DilC_{16} is a lipophilic carbocyanine dye that can be inserted into the membrane to give off the red light. Then the cells were washed and cultured in basal medium stimulated with Ang II (100 ng/ml) for 24 hr. Supernatants were collected and centrifuged to get exosomes. Exosomes were re-suspended in basal medium and added to culture cardiac fibroblasts. After incubation for 48 hr, cardiac fibroblasts were fixed, washed, and viewed with a confocal laser scanning microscope (TCS 4D; Leica).

Transfections

Cardiac fibroblasts were transfected with microON mir-155 mimic (100 nM), microON mir-155 inhibitor (100 nM) and control RNAs using Lipofectamine 2000 according to the manufacturer's instructions. Cells were harvested 48 hr after transfection. Sos1 and control siRNA (100 nM) were performed following the manufacture's guidelines. The efficiency and function assay were confirmed 72 hr after siRNA transfection.

BrdU Staining

Proliferation was measured by BrdU staining as described.[42] Briefly, cardiac fibroblasts were incubated with BrdU (100 nM) for 4 hr and fixed with 4% paraformaldehyde for 10 min at room temperature. Cells were then incubated as follows: 10 min for 0.3% Triton X-100, 1 hr for 2 M hydrochloric acid, and 10 min for antipyonin. After being blocked with serum-free protein block buffer (Dako) for 30 min, cells were incubated with antibodies against BrdU (1:200) at 4°C overnight and then with secondary antibodies (Jackson ImmunoResearch Laboratories) at a 1:500 dilution for 1 hr at room temperature. Images were captured and analyzed by ImageXpress Micro XLS (Molecular Devices).

Plasmid Construction and Luciferase Assay

As it was described previously,[43] the entire mouse Sos1 3′-UTR segment was amplified by PCR using genomic DNA as a template. The PCR product was subcloned into psiCHECK-2 vector following the manufacturer's protocol (Promega). Plasmid DNA was sequenced to ensure its authenticity. 293T cells were cultured in a 96-well plate, and each well was transfected with 0.2 μg luciferase reporter constructs

described above at the same time with microON mir-155 mimic (100 nM) or control RNAs using Lipofectamine 2000 (Invitrogen). After 48 hr, cells were assayed using luciferase assay kits (Promega).

Cytometric Beads Array Assays by Fluorescence Activating Cell Sorting

Cytokine levels were detected by commercially available Cytometric Beads Array kit (CBA, Pharmingen) to quantify mouse IL-1β, IL-6, TNF-α, and MCP-1 (CCL2). The CBA immunoassay was carried out in supernatants of fibroblasts co-cultured with mir-155 mimic and exosomes according to the manufacturer's instruction.[25]

RNA Isolation and Real-Time qPCR

Total RNA was extracted using Trizol reagent method (Invitrogen). Total RNA of 2 μg was reversed to first-strand cDNA with moloney murine leukemia virus reverse transcriptase (Promega). Real-time PCR was performed using 2 μl of reaction mixture with 10 μl SYBR Green PCR Master Mix (Takara) and 1 μmol/L primers. We use a 2-ddCT method to calculate the relative folds of mRNA expression after normalization of the transcript amount to the endogenous control.[44] The housekeeping gene GAPDH and U6 were used as control: expression of mRNA was expressed as a ratio to that of GAPDH and expression of miRNA was expressed as a ratio to that of U6. Melting curve analysis was performed at the end of PCR reaction. The following are the primer sequences: mir-155: reverse transcription (RT) 5′-GTCGTATCCAGTGCGTGTCGTGGAGTCGGCAATTGC ACTGGATACGACACCCCT-3′, forward 5′-GGGGGTTAATGCTA ATTGTGAT-3′ and reverse 5′-AGTGCGTGTCGTGG-3′; U6: RT 5′-CGCTTCACGAATTTGCGTGTCAT-3′, forward 5′-GCTTCGGCA GCACATATACTAAAAT-3′ and reverse 5′-CGCTTCACGAATTT GCGTGTCAT-3′; α-SMA: forward GCCATCTTTCATTGGGAT GGA and Reverse CCCCTGACAGGACGTTGTTA; Col1a: forward CGATGGATTCCCGTTCGAGT and Reverse GAGGCCTCGGTG GACATTAG; Col3a: forward TCCTGGTGGTCCTGGTACTG and reverse AGGAGAACCACTGTTGCCTG; Sos1: forward 5′-GCAG CAGCTGCCTTACGAG-3′ and reverse 5′-TCCTCCACATCTGAA GCACTC-3′; GAPDH: forward 5′-CATGGCCTTCCGTGTTCC TA-3′ reverse 5′-GCGGCACGTCAGATCCA-3′.

Western Blotting Analysis

Western blotting analysis was performed as described.[36] In brief, proteins were extracted from cultured cells or exosomes isolated from macrophages stimulated by PBS, LPS, or AngII with lysis buffer. Protein lysates of 50 μg were separated by 8% SDS-PAGE before transfer to nitrocellulose membranes (Millipore), which were incubated with the primary antibodies anti-Sos1 (1:1,000, Santa Cruz), anti-Socs1 (1:1,000, CST), anti-Alix (1:500), anti-CD68 (1:500), anti-Grp94 (1:1,000), anti-calnexin (1:1000), anti-GM130 (1:1,000), anti-CYC1 (1:1,000), anti-HIST*H* (1:1,000), anti-AGO2 (1:1,000), and anti-GAPDH (1:1,000, Santa Cruz) at 4°C overnight and then with infrared dye-conjugated secondary antibodies (1:10,000; Rockland Immunochemical) for 1 hr at room temperature. The images were quantified by the use of the Odyssey infrared imaging system (LI-COR Biosciences).

Animals and Model of Myocardial Infarction

mir-155$^{-/-}$ mice and littermate WT mice in C57BL/6 background were purchased from The Jackson Laboratory. Mice were given a standard diet and maintained in a pathogen-free animal facility. The Animal Care and Use Committee of Capital Medical University approved all the housing and surgical procedures.

In model of myocardial infarction, 10-week-old male mice were subjected to ligation of left coronary artery (LCA) as described.[45] Mice were sacrificed at the seventh day after post-operation, and heart tissues were harvested. Mice each group were randomly divided for further use.

Histopathology

Immunohistochemical staining was performed as described.[46] Heart tissues were fixed in 4% paraformaldehyde, embedded in paraffin, and sectioned (5 μm). Heart sections were incubated with antibodies against BrdU, collagen I (1:500), and α-SMA (1:200) at 4°C overnight, then with secondary antibodies at room temperature for 30 min and detected with 3,3′-diaminobenzidine for immunohistochemistry. Images were captured by Nikon Eclipse TE2000-S microscope (Nikon) and analyzed by Image Pro Plus 3.1 (Nikon). H&E staining and Masson trichrome staining were carried out as described.[42]

Cell Isolation by Flow Sorting

Macrophages were sorted by CD45$^+$CD11b$^+$; T cells were by CD45$^+$ CD11b$^-$; endothelial cells were by CD45$^-$CD31$^+$; cardiac fibroblasts were by CD45$^-$CD31$^-$PDGFR$^+$; cardiomyocytes were sorted by CD45$^-$CD31$^-$PDGFR$^-$. All the cells were sorted from the heart of myocardial infarction and sham operation by FACSAria II (BD).

Exosome Transfusion Experiment

Starting on the day the acute myocardial infarction was performed as described,[47] saline or exosomes derived from AngII-stimulated WT macrophages (100 or 200 μg) were injected intravenously into mir-155$^{-/-}$ mice every other day for a total four injections. The exosomes were first injected at 30 min before operation, and three followed injections were performed at the day 2, 4, or 6 after myocardial infarction. The mice were sacrificed after 7 days, and the heart were removed, fixed in 4% paraformaldehyde, embedded in paraffin, sectioned, and then stained with Masson trichrome staining.

Statistical Analysis

All values are presented as the mean ± SEM of n independent experiments. Statistical analysis involved one-way ANOVA followed by Bonferroni test for selected pairs with use of GraphPad Prism 5 statistical software. $p < 0.05$ was considered statistically significant.

SUPPLEMENTAL INFORMATION

Supplemental Information includes four figures and can be found with this article online at http://dx.doi.org/10.1016/j.ymthe.2016.09.001.

AUTHOR CONTRIBUTIONS

C.W. designed and conducted all experiments, C.Z. assisted in the pathological staining experiments and CBA, L.L. assisted in the in vivo experiments, X.A. assisted in the the bone-marrow-derived macrophages isolation, B.C. conducted the myocardial infarction model, Y.L. and J.D. guided the experimental design. All authors approved the final manuscript.

ACKNOWLEDGMENTS

We thank Dr. Wenchao Song for critically reading the manuscript. This work was supported by the National Natural Science Foundation of China (grant numbers 81230006, 81470428, and 91539121); the Beijing Natural Science Foundation of China (grant number 7132043); The Key Laboratory of Remodeling-Related Cardiovascular Diseases, Ministry of Education; and the Beijing Collaborative Innovative Research Centre for Cardiovascular Diseases (grant number PXM2014_014226_000002).

REFERENCES

1. Philippen, L.E., Dirkx, E., Wit, J.B., Burggraaf, K., de Windt, L.J., and da Costa Martins, P.A. (2015). Antisense MicroRNA therapeutics in cardiovascular disease: Quo vadis? Mol. Ther. *23*, 1810–1818.
2. Small, E.M., Frost, R.J., and Olson, E.N. (2010). MicroRNAs add a new dimension to cardiovascular disease. Circulation *121*, 1022–1032.
3. Mathivanan, S., Ji, H., and Simpson, R.J. (2010). Exosomes: Extracellular organelles important in intercellular communication. J. Proteomics *73*, 1907–1920.
4. Yellon, D.M., and Davidson, S.M. (2014). Exosomes: Nanoparticles involved in cardioprotection? Circ. Res. *114*, 325–332.
5. Sahoo, S., and Losordo, D.W. (2014). Exosomes and cardiac repair after myocardial infarction. Circ. Res. *114*, 333–344.
6. Waldenström, A., and Ronquist, G. (2014). Role of exosomes in myocardial remodeling. Circ. Res. *114*, 315–324.
7. Loyer, X., Vion, A.C., Tedgui, A., and Boulanger, C.M. (2014). Microvesicles as cell-cell messengers in cardiovascular diseases. Circ. Res. *114*, 345–353.
8. Morello, M., Minciacchi, V.R., de Candia, P., Yang, J., Posadas, E., Kim, H., Griffiths, D., Bhowmick, N., Chung, L.W., Gandellini, P., et al. (2013). Large oncosomes mediate intercellular transfer of functional microRNA. Cell Cycle *12*, 3526–3536.
9. Soo, C.Y., Song, Y., Zheng, Y., Campbell, E.C., Riches, A.C., Gunn-Moore, F., and Powis, S.J. (2012). Nanoparticle tracking analysis monitors microvesicle and exosome secretion from immune cells. Immunology *136*, 192–197.
10. Hulsmans, M., and Holvoet, P. (2013). MicroRNA-containing microvesicles regulating inflammation in association with atherosclerotic disease. Cardiovasc. Res. *100*, 7–18.
11. Zhang, Y., Liu, D., Chen, X., Li, J., Li, L., Bian, Z., Sun, F., Lu, J., Yin, Y., Cai, X., et al. (2010). Secreted monocytic miR-150 enhances targeted endothelial cell migration. Mol. Cell *39*, 133–144.
12. Ismail, N., Wang, Y., Dakhlallah, D., Moldovan, L., Agarwal, K., Batte, K., Shah, P., Wisler, J., Eubank, T.D., Tridandapani, S., et al. (2013). Macrophage microvesicles induce macrophage differentiation and miR-223 transfer. Blood *121*, 984–995.
13. Deng, L., Blanco, F.J., Stevens, H., Lu, R., Caudrillier, A., McBride, M., McClure, J.D., Grant, J., Thomas, M., Frid, M., et al. (2015). MicroRNA-143 activation regulates smooth muscle and endothelial cell crosstalk in pulmonary arterial hypertension. Circ. Res. *117*, 870–883.
14. Vicencio, J.M., Yellon, D.M., Sivaraman, V., Das, D., Boi-Doku, C., Arjun, S., Zheng, Y., Riquelme, J.A., Kearney, J., Sharma, V., et al. (2015). Plasma exosomes protect the myocardium from ischemia-reperfusion injury. J. Am. Coll. Cardiol. *65*, 1525–1536.
15. Fujiu, K., Wang, J., and Nagai, R. (2014). Cardioprotective function of cardiac macrophages. Cardiovasc. Res. *102*, 232–239.
16. Li, Y., Zhang, C., Wu, Y., Han, Y., Cui, W., Jia, L., Cai, L., Cheng, J., Li, H., and Du, J. (2012). Interleukin-12p35 deletion promotes CD4 T-cell-dependent macrophage differentiation and enhances angiotensin II-Induced cardiac fibrosis. Arterioscler. Thromb. Vasc. Biol. *32*, 1662–1674.
17. Berk, B.C., Fujiwara, K., and Lehoux, S. (2007). ECM remodeling in hypertensive heart disease. J. Clin. Invest. *117*, 568–575.
18. Zhang, C., Li, Y., Wang, C., Wu, Y., Cui, W., Miwa, T., Sato, S., Li, H., Song, W.C., and Du, J. (2014). Complement 5a receptor mediates angiotensin II-induced cardiac inflammation and remodeling. Arterioscler. Thromb. Vasc. Biol. *34*, 1240–1248.
19. Heinrichs, D., Knauel, M., Offermanns, C., Berres, M.L., Nellen, A., Leng, L., Schmitz, P., Bucala, R., Trautwein, C., Weber, C., et al. (2011). Macrophage migration inhibitory factor (MIF) exerts antifibrotic effects in experimental liver fibrosis via CD74. Proc. Natl. Acad. Sci. USA *108*, 17444–17449.
20. McNamara, A., Jenne, B.M., and Dean, M.F. (1985). Fibroblasts acquire beta-glucuronidase by direct and indirect transfer during co-culture with macrophages. Exp. Cell Res. *160*, 150–157.
21. Heymans, S., Corsten, M.F., Verhesen, W., Carai, P., van Leeuwen, R.E., Custers, K., Peters, T., Hazebroek, M., Stöger, L., Wijnands, E., et al. (2013). Macrophage microRNA-155 promotes cardiac hypertrophy and failure. Circulation *128*, 1420–1432.
22. O'Connell, R.M., Taganov, K.D., Boldin, M.P., Cheng, G., and Baltimore, D. (2007). MicroRNA-155 is induced during the macrophage inflammatory response. Proc. Natl. Acad. Sci. USA *104*, 1604–1609.
23. Tili, E., Michaille, J.J., Cimino, A., Costinean, S., Dumitru, C.D., Adair, B., Fabbri, M., Alder, H., Liu, C.G., Calin, G.A., and Croce, C.M. (2007). Modulation of miR-155 and miR-125b levels following lipopolysaccharide/TNF-alpha stimulation and their possible roles in regulating the response to endotoxin shock. J. Immunol. *179*, 5082–5089.
24. Depeille, P., Henricks, L.M., van de Ven, R.A.H., Lemmens, E., Wang, C.Y., Matli, M., Werb, Z., Haigis, K.M., Donner, D., Warren, R., and Roose, J.P. (2015). RasGRP1 opposes proliferative EGFR-SOS1-Ras signals and restricts intestinal epithelial cell growth. Nat. Cell Biol. *17*, 804–815.
25. Zhang, J., Xiao, Z., Qu, C., Cui, W., Wang, X., and Du, J. (2014). CD8 T cells are involved in skeletal muscle regeneration through facilitating MCP-1 secretion and Gr1(high) macrophage infiltration. J. Immunol. *193*, 5149–5160.
26. Huffaker, T.B., and O'Connell, R.M. (2015). miR-155-SOCS1 as a functional axis: Satisfying the burden of proof. Immunity *43*, 3–4.
27. Shinde, A.V., and Frangogiannis, N.G. (2014). Fibroblasts in myocardial infarction: A role in inflammation and repair. J. Mol. Cell. Cardiol. *70*, 74–82.
28. Curtis, A.M., Fagundes, C.T., Yang, G., Palsson-McDermott, E.M., Wochal, P., McGettrick, A.F., Foley, N.H., Early, J.O., Chen, L., Zhang, H., et al. (2015). Circadian control of innate immunity in macrophages by miR-155 targeting Bmal1. Proc. Natl. Acad. Sci. USA *112*, 7231–7236.
29. He, W., Huang, H., Xie, Q., Wang, Z., Fan, Y., Kong, B., Huang, D., and Xiao, Y. (2016). MiR-155 knockout in fibroblasts improves cardiac remodeling by targeting tumor protein p53-Inducible nuclear protein 1. J. Cardiovasc. Pharmacol. Ther. *21*, 423–435.
30. Corsten, M.F., Papageorgiou, A., Verhesen, W., Carai, P., Lindow, M., Obad, S., Summer, G., Coort, S.L., Hazebroek, M., van Leeuwen, R., et al. (2012). MicroRNA profiling identifies microRNA-155 as an adverse mediator of cardiac injury and dysfunction during acute viral myocarditis. Circ. Res. *111*, 415–425.
31. Lv, Z., and Yang, L. (2013). MiR-124 inhibits the growth of glioblastoma through the downregulation of SOS1. Mol. Med. Rep. *8*, 345–349.
32. Xu, C.C., Zheng, L., Chen, W.D., Ruan, C.C., Zhu, D.L., and Gao, P.J. (2009). MicroRNA-155 regulates angiotensin II type 1 receptor expression and phenotypic differentiation in vascular adventitial fibroblasts. Int. J. Cardiol. *137*, S141–S142.
33. Yang, Y., Yang, L., Liang, X., and Zhu, G. (2015). MicroRNA-155 promotes atherosclerosis inflammation via targeting SOCS1. Cell. Physiol. Biochem. *36*, 1371–1381.
34. Porter, K.E., and Turner, N.A. (2009). Cardiac fibroblasts: At the heart of myocardial remodeling. Pharmacol. Ther. *123*, 255–278.

35. Buckley, C.D., Pilling, D., Lord, J.M., Akbar, A.N., Scheel-Toellner, D., and Salmon, M. (2001). Fibroblasts regulate the switch from acute resolving to chronic persistent inflammation. Trends Immunol. *22*, 199–204.

36. Wu, Y., Li, Y., Zhang, C., A, X., Wang, Y., Cui, W., Li, H., and Du, J. (2014). S100a8/a9 released by CD11b+Gr1+ neutrophils activates cardiac fibroblasts to initiate angiotensin II-Induced cardiac inflammation and injury. Hypertension *63*, 1241–1250.

37. Stanczyk, J., Pedrioli, D.M., Brentano, F., Sanchez-Pernaute, O., Kolling, C., Gay, R.E., Detmar, M., Gay, S., and Kyburz, D. (2008). Altered expression of MicroRNA in synovial fibroblasts and synovial tissue in rheumatoid arthritis. Arthritis Rheum. *58*, 1001–1009.

38. Mishina, H., Watanabe, K., Tamaru, S., Watanabe, Y., Fujioka, D., Takahashi, S., Suzuki, K., Nakamura, T., Obata, J.E., Kawabata, K., et al. (2014). Lack of phospholipase A2 receptor increases susceptibility to cardiac rupture after myocardial infarction. Circ. Res. *114*, 493–504.

39. Matsui, Y., Ikesue, M., Danzaki, K., Morimoto, J., Sato, M., Tanaka, S., Kojima, T., Tsutsui, H., and Uede, T. (2011). Syndecan-4 prevents cardiac rupture and dysfunction after myocardial infarction. Circ. Res. *108*, 1328–1339.

40. Frangogiannis, N.G. (2012). Regulation of the inflammatory response in cardiac repair. Circ. Res. *110*, 159–173.

41. Lake, F.R., Noble, P.W., Henson, P.M., and Riches, D.W. (1994). Functional switching of macrophage responses to tumor necrosis factor-alpha (TNF alpha) by interferons. Implications for the pleiotropic activities of TNF alpha. J. Clin. Invest. *93*, 1661–1669.

42. Calkins, M.J., and Reddy, P.H. (2011). Assessment of newly synthesized mitochondrial DNA using BrdU labeling in primary neurons from Alzheimer's disease mice: Implications for impaired mitochondrial biogenesis and synaptic damage. Biochim. Biophys. Acta *1812*, 1182–1189.

43. Cheng, J., and Du, J. (2007). Mechanical stretch simulates proliferation of venous smooth muscle cells through activation of the insulin-like growth factor-1 receptor. Arterioscler. Thromb. Vasc. Biol. *27*, 1744–1751.

44. Hwang, K.C., Park, S.Y., Park, S.P., Lim, J.H., Cui, X.S., and Kim, N.H. (2005). Specific maternal transcripts in bovine oocytes and cleavaged embryos: Identification with novel DDRT-PCR methods. Mol. Reprod. Dev. *71*, 275–283.

45. Gao, E., Lei, Y.H., Shang, X., Huang, Z.M., Zuo, L., Boucher, M., Fan, Q., Chuprun, J.K., Ma, X.L., and Koch, W.J. (2010). A novel and efficient model of coronary artery ligation and myocardial infarction in the mouse. Circ. Res. *107*, 1445–1453.

46. Jia, L.X., Zhang, W.M., Zhang, H.J., Li, T.T., Wang, Y.L., Qin, Y.W., Gu, H., and Du, J. (2015). Mechanical stretch-induced endoplasmic reticulum stress, apoptosis and inflammation contribute to thoracic aortic aneurysm and dissection. J. Pathol. *236*, 373–383.

47. Li, J., Zhang, Y., Liu, Y., Dai, X., Li, W., Cai, X., Yin, Y., Wang, Q., Xue, Y., Wang, C., et al. (2013). Microvesicle-mediated transfer of microRNA-150 from monocytes to endothelial cells promotes angiogenesis. J. Biol. Chem. *288*, 23586–23596.